Catalysis Letters 62 (1999) 59–65

SO_4–ZrO_2 catalysts for the esterification of benzoic acid to methylbenzoate

S. Ardizzone, C.L. Bianchi, V. Ragaini and B. Vercelli

Department of Physical Chemistry and Electrochemistry, University of Milan, Via Golgi 19, 20133 Milan, Italy

Received 22 December 1998; accepted 29 July 1999

SO_4–ZrO_2 catalysts, prepared by varying the conditions of oxide preparation and H_2SO_4 impregnation, have been characterized by means of different techniques (XRD, BET, Hammett–Bertolacini technique, XPS). The esterification of benzoic acid to methylbenzoate has been used to test the different catalysts and their catalytic performance has been discussed in the light of their bulk and surface properties.

Keywords: SO_4–ZrO_2 catalysts, esterification reactions, XPS data

1. Introduction

In recent years the development of solid acid catalysts which might efficiently replace, in several industrial processes, strong liquid acids (as H_2SO_4 and HF) has been the object of active research. In fact solid catalysts, being less corrosive and easier to separate from the reaction products, may become more advantageous and are intrinsically more compatible with the increasingly demanding environmental requirements [1–12].

SO_4–ZrO_2 powders find large applications as "superacid" catalysts in several reactions and mainly in selective hydrocarbon isomerization [13–27]. These compounds are active in hydrocarbon conversion at temperatures lower than the most of the generally used solid catalysts. In respect to zeolite, sulfated zirconia allows the same hydrocarbon conversion level to be obtained at temperatures from 100 to 200 K lower [27,28]. In our laboratory recently [26] the isomerization efficiency of SO_4–ZrO_2 powders, coupled with traditional Fischer–Tropsch catalysts, was found to be a direct function of the surface density of the more acid sites of the catalyst.

The activity of SO_4–ZrO_2 powders as heterogeneous catalysts in liquid media has been less investigated. Recently, appreciable activity of SO_4–ZrO_2 for the hydrolysis of esters in the presence of water was reported [1,2].

In the present work SO_4–ZrO_2 powders are used as heterogeneous catalysts for the esterification of benzoic acid with methanol, which is usually performed with catalysts in homogeneous phase like mineral acids (sulfuric and hydrochloric ones) or the less active and corrosive alchilsulphonic acids (*p*-toluenesulphonic acid (PTS)).

The aim of the present work is to study the role played by the features of the catalysts (e.g., preparation conditions, degree of acidity, etc.) on the trend of the heterogeneous reaction. SO_4–ZrO_2 samples have been prepared in the laboratory and show different bulk and surface features. The catalytic tests are discussed in the light of the results of acidity characterization (by a modification of the Hammett–Bertolacini approach) and of surface chemical state (by XPS spectroscopy) performed both on "fresh" and on "exhausted" powders.

2. Experimental

All the chemicals were of reagent grade purity and were used without further purification; doubly distilled water passed through a Milli-Q apparatus was used to prepare solutions and suspensions.

2.1. Catalyst preparation

SO_4–ZrO_2 were prepared by calcining at 743 K for 5 h hydrous zirconia precursors obtained, following a previously reported pathway [29,30] consisting in the hydrolysis, at the boiling point, of $ZrCl_4$ acid solutions, by KOH dropwise additions (about 60 drops/min) under vigorous stirring. The pH of the suspensions was changed in the range between 6.2 and 12.3 to obtain precursors with different features. The products of the precipitation reaction, purified by centrifugation/resuspension, were dried and stored as a powder.

The samples were treated with H_2SO_4, by equilibration of the powders in the solutions at room temperature and under stirring for 1 h by varying the concentration of the acid (5×10^{-1} and 1 M) and keeping solution volume to the powder weight constant (16.5 ml g^{-1}). Only one sample (F2) was prepared by adopting a higher H_2SO_4 volume/weight ratio (33 ml g^{-1}). The solids were then filtered, dried at 473 K and successively calcined at 743 K for 5 h.

Table 1 reports the presently prepared samples together with the relative conditions of preparation and H_2SO_4 impregnation.

Table 1
Characterizations of un-doped and H_2SO_4-impregnated ZrO_2 precursors calcined at 743 K.[a]

Sample	Precip.	Phase composition[b] (%)		S_{BET}	$[H_2SO_4]$
	pH	Monoclinic	Tetragonal	($m^2\,g^{-1}$)	($mol\,l^{-1}$)
A	6.0	50	50	89	Un-doped
A1	6.0	0	100	207	5×10^{-1}
A2	6.0	0	100	192	1
B	6.2	80	20	71	Un-doped
B2	6.2	0	100	162	1
C	7.2	60	40	117	Un-doped
C1	7.2	0	100	194	5×10^{-1}
D	7.6	0	100	116	Un-doped
D2	7.6	0	100	226	1
E	9.3	0	100	115	Un-doped
E1	9.3	0	100	214	5×10^{-1}
F	10.3	0	100	121	Un-doped
F2	10.3	0	100	138	1
G	12.3	0	100	175	Un-doped
G1	12.3	0	100	250	5×10^{-1}
G2	12.3	0	100	220	1

[a] The H_2SO_4 impregnation was performed before calcination.
[b] In the case of mixed phase samples the relative enrichment in the two polymorphs was evaluated on the basis of the Toraya model [38].

Few samples were recovered after the catalytic test and "washed" by ten cycles centrifugation and resuspension in pure ethanol.

2.2. Catalyst characterization

Structural characterization of the powders was performed by X-ray diffraction, by means of a Siemens D500, using nickel filtered Co and Cu radiation. Specific surface areas were determined by adsorption of N_2 at low temperatures (BET technique) using a Coulter SA3100 apparatus.

XPS spectra were obtained using an M-probe apparatus (Surface Science Instruments). The source was monochromatic Al K_α radiation (1486.6 eV). A spot size of 200×750 μm and a pass energy of 25 eV were used. The energy scale was calibrated with reference to the $4f_{7/2}$ level of a freshly evaporated gold sample, at 84.00 ± 0.1 eV, and with reference to the $2p_{3/2}$ and 3s levels of copper at 932.47 ± 0.1 and 122.39 ± 0.15 eV, respectively; 1s level hydrocarbon-contaminant carbon was taken as the internal reference at 284.6 eV. The position and FWHM of the C 1s line were checked carefully for every independent determination. The accuracy of the reported binding energies (BE) can be estimated to be ± 0.2 eV. The curve fitting program mixes Gaussian and Lorentzian curves and allows the asymmetry parameter to vary from 0 to 100%. In the present case all the curves were fitted by 100% Gaussian peaks.

The surface acidity features of the following samples were determined by a modification of the Hammett–Bertolacini (HB) technique [31–33]. This method, described in detail in [26,33], relies on the selective adsorption of dye molecules, with different pK_a values, on the oxide surface.

2.3. Catalyst leaching

Determinations of SO_4^{2-} possibly leached from the catalysts during the course of the reaction have been performed.

Samples have been withdrawn from the reaction mixture at different times. The sampled suspensions were diluted with benzene and kept at 323 K to prevent crystallization of benzoic acid and subsequently shaken with water (always at 323 K) to promote partition of sulfates into the polar solvent.

Sulfates have been searched by HPLC using an HP 1050 instrument with a gradient quaternary pump and an UV detector. The method detection limit is: $SO_4^{2-} < 0.5$ ppm.

To further assess the heterogeneous role of the present catalysts some selected experiments were performed by separating the solid catalyst from the reaction mixture and measuring the ensuing product conversions in the absence of zirconia powders.

2.4. Catalytic performance

The esterification reaction of the benzoic acid to methylbenzoate with methanol was chosen to test the catalytic efficiency of the sulfated zirconia samples.

As the esterification reaction is an equilibrium one, a particular experimental procedure, which permits to shift the equilibrium to the reaction product (methylbenzoate), has been realized by selecting a reaction temperature, 430 ± 1 K, which provokes the continuous distillation of water, produced during the reaction. As the boiling point of methanol is 338 K, the operative way may be described as a modified "batch process", where the reagents are put altogether in the reactor and methanol is continuously added and taken off together with water. In this way, high conversions in short reaction times (8 h) have been obtained, so that the process becomes interesting for industrial application.

The reaction was performed by adding equal amounts of the reactants (about 3 moles of each) in the reactor, with a little quantity of the product of the reaction (about 10% of the benzoic acid weight) to keep the carboxylic acid in solution.

3.2 g of catalyst were added in the reactor and drawings of 5 ml of the reaction moisture at 2, 4, 5, 6.5 and 8 h were made to test the catalytic performance. To assess the reproducibility of the catalytic activity of the powders, separate runs using the same catalysts were performed.

Results are presented as conversion percentages of benzoic acid as a function of time and have been obtained by titrating the unreacted benzoic acid with a 1 N standard solution of NaOH using phenolphthalein as colorimetric indicator. The accuracy of the reported catalytic conversion data can be estimated to be $\pm 0.5\%$. This value takes into account both the reproducibility of the catalytic activity and the accuracy of the analytical method.

3. Results and discussion

3.1. Catalytic tests

Leaching tests aimed at verifying the possible release of sulfates from the catalysts during the course of the reaction were in any case negative, i.e., no sulfates were found in the suspension within the limit of detection of the technique (<0.5 ppm). To further exclude an homogeneous catalytic mechanism, several tests were performed by separating the solid catalyst from the reaction mixture. In all cases the filtrate presented no catalytic activity. Consequently, in the following, the catalysis will be considered as heterogeneous.

Figure 1 reports the course of the esterification reaction over a variety of SO_4–ZrO_2 catalysts. The figure reports also, by comparison, the trend observed in the absence of catalyst. The reagent conversion increases steadily with the reaction time approaching quasi-plateau values for 450–480 min reaction time length. The various catalysts show large differences particularly at short reaction times as, at 120 min, the conversion varies from 44–45% for the best catalysts to 13% for the least efficient one. For longer reaction times the catalyst effects are less marked and variations fall within 65 and 80% reagent conversion. The conversion sequence at short reaction times (120 min) shown by the different oxide powders is the following:

$$F2 > D2 > A1 > A2 > C1 > B2 > E1 > G1 > G2.$$

The sequence can be compared with the outcome of first-order plots. In the coordinates of the integrated rate law (figure 2) the points pertaining to the first five catalysts of the sequence, are grouped around a single line (figure 2, line labeled as (∗)) which yields a rate constant, k, of 2.5×10^{-5} s^{-1}. The linear correlation is acceptable in the case of samples A1, D2, A2 and C1 (around 0.98) while it is poor in the case of sample F2 (0.941) (see the dotted curve in the figure). The less efficient catalysts yield lines with decreasing slopes but with poor correlation coefficients (0.95–0.88). The trend shown by some of the less efficient catalysts is reported in the figure, in the absence of experimental points to avoid confusions.

Collectively the samples which show larger deviations from the first-order law are G1, G2, E1, C1 and F2.

The catalyst efficiency sequence at short reaction time (120 min) and the quality of the agreement to a first-order law can be discussed on the grounds of the oxide features reported in tables 1 and 2.

Table 1 reports the data concerning the phase composition and specific surface area characterizations together with the pH of precipitation of each precursor. Results refer to calcined (5 h, 743 K) samples both un-doped (in the absence of H_2SO_4 treatment), for the sake of comparison, and acid "doped". All the H_2SO_4-treated samples appear to be purely metastable (tetragonal).

Table 2 presents the density of the acid sites at the surfaces of the catalysts for each pK_a value.

The role played by the pH of precipitation of the hydrous zirconia precursor will be commented first, this being one of the key parameters affecting the phase composition of the calcined oxide. In fact, it is generally reported that the more alkaline the precipitation pH is, the richer in tetrago-

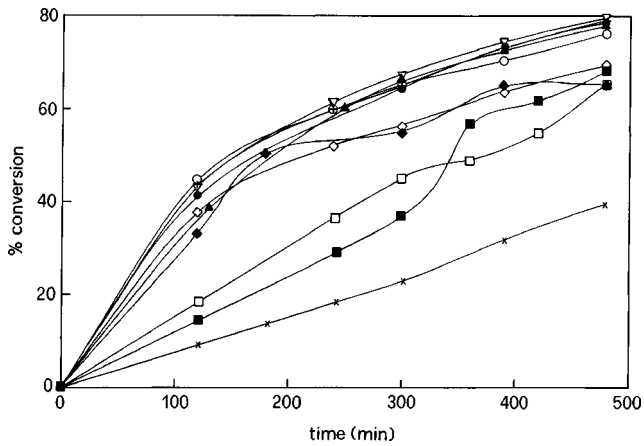

Figure 1. Time courses for the esterification of benzoic acid to methylbenzoate over different SO_4–ZrO_2 catalysts: (▽) A1, (●) A2, (▲) B2, (◇) C1, (+) D2, (♦) E1, (○) F2, (□) G1, (■) G2. The (×) curve refers to the reaction performed in the absence of catalyst.

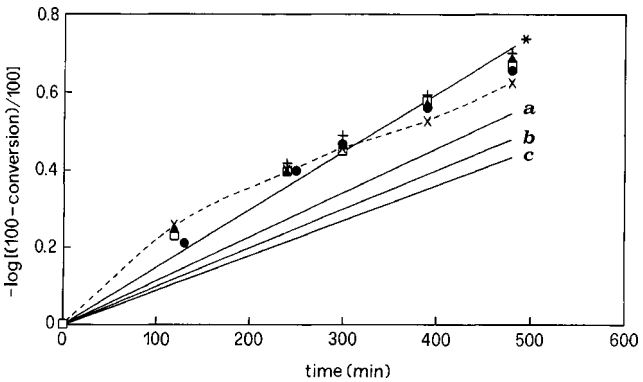

Figure 2. First-order plots for the esterification of benzoic acid to methylbenzoate over different SO_4–ZrO_2 catalysts. The line labeled by (∗) represents F2, A1, D2, A2 and B2 samples. The dotted curve connecting points relative to F2 powders shows the poor agreement of these data to a first-order law. Lines (a), (b) and (c) are relative to samples C1, G2 and G1, respectively.

Table 2
Density of the sites at each pK_a for all the SO_4–ZrO_2.

Sample	Number of sites[a] (μeq)				
	pK_a −14.2	pK_a −8.2	pK_a −5.6	pK_a −3	pK_a 1.5
A1	–	1393	2389	–	–
A2	1597	–	1122	–	–
B2	2623	–	–	2234	–
C1	–	–	1182	–	–
D2	2217	–	1900	–	–
E1	2195	–	732	–	–
F2	2327	–	1375	–	–
G1	–	–	–	–	3988
G2	–	–	–	–	3142

[a] Sites present in the reaction mixture, i.e., in 3.2 g of catalyst.

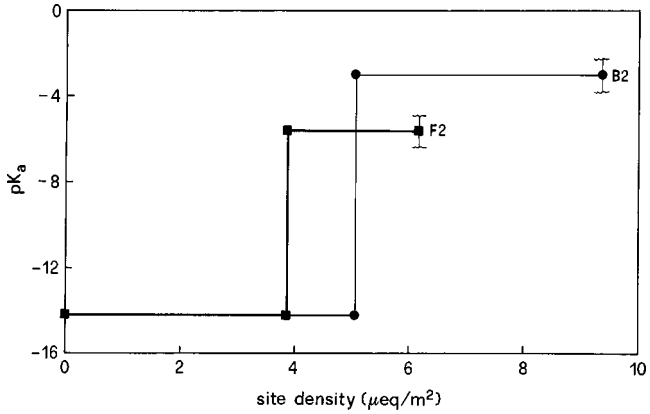

Figure 3. Surface site densities of F2 and B2 samples relative to different pK_a values.

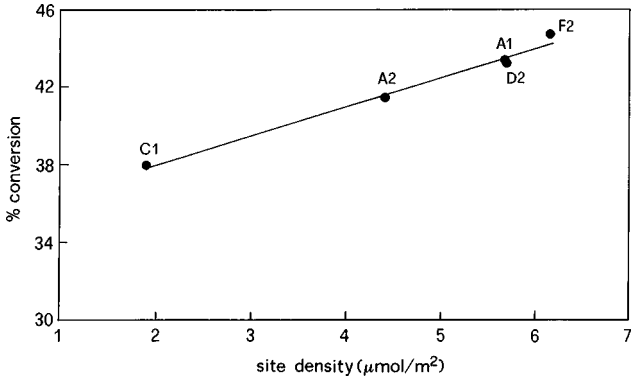

Figure 4. Reagent conversion as a function of the sum of the density of $pK_a = -14.2$ and -5.6 surface sites.

nal (metastable) component is the calcined, un-doped oxide, as in the present case (table 1) [17]. Further the literature is rich in catalytic data (mainly concerning gas-phase reactions) where the conditions of preparation treatment of the oxide are reported to play a key role in affecting the activity of the material [20,26].

At variance with literature data, in the present case the catalyst performance is not related with either pH of precipitation or phase composition of the ZrO_2 polymorphs, the samples obtained at the more alkaline pH (G1, G2), and fully metastable (even in the absence of sulfuric acid treatment) being the last of the sequence. However, one observation can be made: the samples obtained at alkaline pH (G1, G2, E1, F2) are the ones which present larger deviations from the linear first-order kinetic law just as though, in the case of these samples, the reaction might follow a different kinetic pathway.

Besides the phase composition, the acidity degree of the samples (in its turn strictly connected with the phase composition) is generally in direct relation with the catalyst efficiency [26].

Also in this respect the present reaction is atypical: the catalyst efficiency does not reflect the sequence of either of the total number of acid sites or of the number of the most acid sites ($pK_a = -14.2$) (see table 2). The three top (F2, D2, A1) catalysts show small catalytic differences in efficiency between one another and have comparable total number of sites, but are not the samples showing either the maximum number of total sites (B2, G1) or the maximum number of most acid sites (B2). As an example figure 3 reports the comparison between the acid features of sample B2, the sixth in the short time conversion sequence, and of sample F2, the best catalyst. Sample B2 shows a higher density of most acid sites ($pK_a = -14$) and a higher total density of sites with respect to sample F2 but is not, however, one of the top catalysts.

In the present case the catalytic action of the solid is not an aspecific function of the degree of acidity of the powders; a more close comparison between the data in table 2 and the catalytic sequence shows that the efficiency is the result of a complex interplay between sites with acidity in the range comprised between $pK_a = -5.6$ and -14.2. Figure 4 reports the conversion at 120 min of the five top catalysts as a function of their density of sites in the range $pK_a = -14.2$ and -5.6. It can be observed that the samples show an ordered sequence of increased conversion with increasing the specific site densities. For the less efficient catalysts (B2, E1, G1, G2), either showing a low density of $pK_a = -5.6$ sites or no $pK_a = -5.6$ sites at all, the higher density of more acid sites becomes the sequence parameter.

The sites showing pK_a in the range -5.6 and -8.2 play a key role in the reaction (only sample A1 shows sites at $pK_a = -8.2$). The specific action of the sites at $pK_a = -5.6$ is to be related in the present case to the "chemistry" of the reaction. In fact it is to be recalled that the indicator "selective" for the sites at $pK_a = -5.6$ is benzalacetophenone and for the sites at $pK_a = -8.2$ anthraquinone, both molecules showing apparent similarities with the present reaction reactants and products. These specific sites, therefore, might act as preferential adsorption sites for the reaction intermediates.

The differences between the activity of the catalysts at 480 min reaction time are less marked than at the beginning of the process and the final conversion sequence, for the various samples, is somewhat modified in respect to the one at short reaction time. The activity of the oxides, after 8 h reaction time, cannot be commented on the grounds of characterizations of the samples in the "as-prepared" conditions, as the state of the catalyst surface can be appreciably modified in comparison to the "fresh" oxide. Consequently, also in order to get further support on the nature of the sites active for the reaction, characterizations of catalysts recovered at the end of the reaction have been performed by both the HB technique and XPS analyses.

3.2. "Exhausted" catalyst characterizations

The acidity features obtained upon characterization of the "fresh" and "exhausted" F2 sample, by the HB technique, are reported in figure 5. The figure reports the density of the surface sites relative to the specific pK_a values. It can be noted that the total site density has undergone

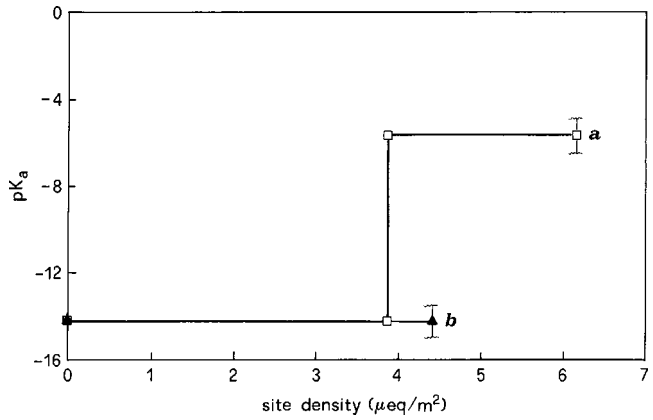

Figure 5. Surface site densities of F2 samples, in the as-prepared, "fresh" conditions, curve (a) and recovered after 8 h reaction time, "exhausted", curve (b).

a decrease of about 30% at the end of the reaction time. The observed total site density decrease, which is not small, might represent only a rather rough estimate of the actual value, due to the invariance of the powder surface area assumed in the density calculations. In fact the amount of powder recovered at the end of the reaction and after submitting it to the purifying cycles was too small to allow a direct determination of its actual surface area to be performed.

A very interesting aspect concerns the speciation of the surface sites: in the "exhausted" sample all the $pK_a = -5.6$ sites have been "consumed" and this is in agreement with the key role already envisaged for these sites in the reaction; apparently these sites are the place for strong chemisorption reactions of either the reactants or the intermediates. These reactions are such as to "block" the $pK_a = -5.6$ sites and give rise to surface rearrangements; in fact, unexpectedly, the density (slightly less than 15% over the initial value) of the $pK_a = -14.2$ sites increases in the "exhausted" catalyst.

This unexpected trend finds direct support from the comparison between Zr 3d XPS spectra obtained in the case of the "fresh" (figure 6(b)) and "exhausted" F2 powders (figure 6(c)). The figure reports also, for the sake of comparison, the Zr 3d doublet for the same un-doped, calcined, oxide precursor (figure 6(a)). This latter figure shows the regular 3d doublet, with BE (182.1 and 184.5 eV) in agreement with literature results for Zr(IV) in the oxide [35]. The Zr 3d peak in figure 6(b) is typical for SO_4–ZrO_2 powders and has been reported previously [26,36,37]. The peak is broad, in respect to the "simple" Zr(IV) doublet, and a one-component curve fitting yields no acceptable results. The peak in figure 6(b) is best fitted by assuming the presence of two zirconium(IV) components: the lower BE component pertains to Zr(IV) in the oxide while the higher energy component corresponds to the formation of a Zr(IV) bound to a more electron-attracting species (BE, 183.5 eV), a sulfur-containing species, although not a $Zr(SO_4)_2$ (184.5 eV [34,35]). The Zr 3d peak of the "exhausted" catalyst (figure 6(c)) can be best fitted by following the same procedure. The shape of the peak in figure 6(c) is even more distorted, when compared to the simple doublet, than the one of the "fresh" catalyst, showing a greater weight of the sulfur-bound zirconium component. The increase in the intensity of the higher energy component of the "exhausted" catalyst in respect to the "fresh" one is of about 20%. This variation can be considered to reflect the observed increase of the degree of acidity (bigger number of $pK_a = -14.2$ sites) of the "exhausted" catalyst, apparent in the HB plot (figure 5). In fact a close connection between the relative weight of the higher energy component of the Zr XPS peak and the degree of acidity of the sample, as expressed by the density/number of $pK_a = -14.2$ sites, has been previously reported [26,37].

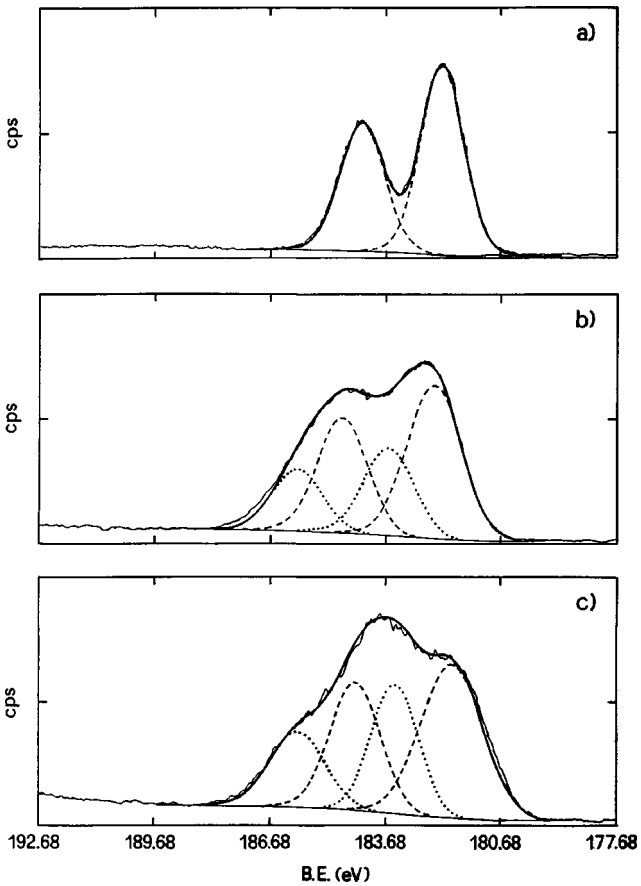

Figure 6. XPS spectra of Zr 3d doublet. (a) Sample F2, calcined, un-doped precursor, (b) "fresh" F2 sample and (c) "exhausted" F2 sample.

A summary of all the XPS features of both "fresh" and "exhausted" F2 sample is reported in table 3. The three kinds of oxygen species resulting from the fitting procedure can be attributed, respectively, to oxygen in the oxide (530.2 and 530.0 eV), oxygen in sulfates (531.7 and 531.4 eV) and to chemisorbed water (533.0 and 532.8 eV) as already reported for sulfated zirconia samples [36]. Both samples showed a single C 1s peak relative to adventitious carbon (284.6 eV). However, it is interesting to observe the C/Zr ratio appears to increase in passing from the "fresh" to the "exhausted" sample.

Table 3
XPS BE (eV) of Zr 3d, O 1s, S 2p and C 1s/Zr 3d atomic ratio for the "fresh" and "exhausted" F2 catalyst.

Sample	Zr[a]		O 1s	S 2p	C/Zr
	$3d_{5/2}$	$3d_{3/2}$			
F2 "fresh"	182.4 (1.60)	184.8 (1.62)	530.2		
			531.7	169.7	0.45
	183.6 (1.63)	186.0 (1.65)	533.0		
F2 "exhausted"	182.1 (1.76)	184.6 (1.61)	530.0		
			531.4	169.6	1.00
	183.5 (1.54)	186.0 (1.89)	532.8		

[a] In parentheses FWHM (full width half maximum) for Zr 3d peaks.

4. Conclusions

SO_4–ZrO_2 catalysts obtained by modulating the conditions of the oxide preparation and of H_2SO_4 impregnation have been tested with respect to the esterification of benzoic acid. The various samples show different catalytic performance, the more so at short reaction times. The total conversion after 8 h reaction time varies between 65 and 80% reagent conversion. The reaction appears to follow a first-order rate law, the agreement being the better the more efficient the catalysts are.

The conversion sequence of the various catalysts at short reaction time (120 min) shows that the performance does not depend either on the conditions of the oxide preparation or on the concentration of the sulfuric acid used in the treatment. Further the catalytic activity towards the present reaction appears not to be a simple function of the degree of acidity of the sample (as total number of acid sites, or total number of the most acid sites, $pK_a = -14.2$).

A close comparison between the results of catalytic activity and of acid characterization shows that the sites at $pK_a = -5.6$ play a key role in the reaction and that the better catalysts are the ones showing the largest density of the sites with pK_a in the range -14.2 and -5.6.

Interesting data emerge from the characterization of an "exhausted" catalyst, recovered after 8 h reaction time. By comparison of the HB data of the "fresh" and "exhausted" sample the following observations can be made:

(i) the total density of sites is reduced by about 30%;

(ii) all the $pK_a = -5.6$ sites have been consumed;

(iii) the density of the $pK_a = -14.2$ sites is slightly increased (about 15%).

This latter increase finds direct support from the parallel increase of the higher BE component of the Zr 3d XPS peak of the "exhausted" catalyst with respect to the "fresh" one.

The key role played by the density of sites at $pK_a = -5.6$, in the present reaction, can be related to the heterogeneous nature of this catalytic process. Apparently the $pK_a = -5.6$ sites represent a preferential locus of adsorption for the reaction intermediates. The adsorption–desorption reactions provoke, in turn, rearrangements of the stoichiometric structure of the surface inducing the observed slight increase of the most acid site density.

Acknowledgement

Dr. Carvoli (Chemial S.p.A.) is acknowledged by the authors for fruitful discussions throughout this work. Financial support from the Ministry of University and Scientific-Technological Research MURST (60 and 40% research Founds) is gratefully acknowledged.

References

[1] T. Okuhara, M. Kimura and T. Nakato, Appl. Catal. A 155 (1997) L9.
[2] M. Kimura, T. Nakato and T. Okuhara, Appl. Catal. A 165 (1997) 227.
[3] K. Tanabe, Appl. Catal. A 113 (1994) 147.
[4] R. Scheldon, CHEMTECH (1991) 566.
[5] S. Namba, N. Hosonuma and T. Yashima, J. Catal. 72 (1981) 16.
[6] M. Kono, Y. Fukuoka, O. Mitsui and H. Ishida, Nippon Kagaku Kaishi (1989) 521.
[7] K. Segawa, A. Suogiyama and Y. Kurusu, Stud. Surf. Sci. Catal. 60 (1991) 73.
[8] A. Kawada, S. Mitamura and S. Kobayashi, J. Chem. Soc. Chem. Commun. (1993) 1157.
[9] T. Okuhara, N. Mizun and M. Misono, Adv. Catal. 41 (1995) 113.
[10] T. Okuhara, T. Nishimura, H. Watanabe and M. Misono, J. Mol. Catal. 74 (1992) 247.
[11] Y. Tanabe, Hydrocarbon Process. (1981) 187.
[12] F.J. Waller and V.S.R. Warren, CHEMTECH 17 (1987) 187.
[13] K. Arata and M. Hino, Mater. Chem. Phys. 26 (1990) 213.
[14] T. Yamaguchi, Appl. Catal. 61 (1990) 1.
[15] G.K. Chuah, S. Jaenicke, S.A. Cheong and K.S. Chang, Appl. Catal. A 145 (1996) 267.
[16] R.P. Denkewiez, Jr., K.S. Tenhuisen and J.H. Adair, J. Mater. Res. 5 (1990) 2698.
[17] A. Clearfield, G.P.D. Serrette and A.H. Khazi-Syed, Catal. Today 20 (1994) 295.
[18] T. Yamaguchi, K. Tanabe and Y.C. Kung, Mater. Chem. Phys. 16 (1986) 67.
[19] R. Srinivasan, D. Taulbee and B.H. Davis, Catal. Lett. 9 (1991) 1.
[20] J.M. Parera, Catal. Today 15 (1992) 481.
[21] R. Srinivasan and B.H. Davis, Catal. Lett. 14 (1992) 165.
[22] M. Waquif, J. Bachelier, O. Saur and J.C. Lavalley, J. Mol. Catal. 72 (1992) 127.
[23] X. Song and A. Sayari, CHEMTECH August (1995) 27.
[24] K. Arata, Appl. Catal. A 146 (1996) 3.
[25] B.H. Davis, R.A. Keogh and R. Srinivasan, Catal. Today 20 (1994) 219.
[26] S. Ardizzone, C.L. Bianchi, W. Cattagni and V. Ragaini, Catal. Lett. 49 (1997) 193.
[27] M. Stocker, J. Mol. Catal. 29 (1985) 371.
[28] M. Hino, S. Kobayashi and K. Arata, J. Am. Chem. Soc. 101 (1979) 6439.
[29] S. Ardizzone, G. Bassi and G. Liborio, Colloids Surf. 51 (1990) 207.
[30] S. Ardizzone, C.L. Bianchi, S. Carella and M.G. Cattania, Mater. Chem. Phys. 34 (1993) 154.
[31] R.J. Bertolacini, Anal. Chem. 35 (1963) 599.
[32] L. Forni, Catal. Rev. 8 (1974) 65.
[33] S. Ardizzone, C.L. Bianchi and B. Vercelli, Appl. Surf. Sci. 126 (1998) 169.
[34] K. Arata, Mater. Chem. Phys. 26 (1990) 213.

[35] J.F. Moulder, W.F. Stickle, P.E. Sobol and K.D. Bomben, in: *Handbook of X-ray Photoelectron Spectroscopy*, ed. J. Chastain (Perkin Elmer Corporation, US, 1992).
[36] S. Ardizzone, C.L. Bianchi and E. Grassi, Colloids Surf. 135 (1998) 41.
[37] S. Ardizzone, C.L. Bianchi and M. Signoretto, Appl. Surf. Sci., in press.
[38] H. Toraya, M. Yoshimura and S. Somiya, J. Am. Ceram. Soc. 60 (1938) 309.